§28. Effect of EBW Heating at Very Low Magnetic Field on Plasma Confinement and MHD Characteristics in the Heliotron J

Takahashi, H., Toi, K., Igami, H., Yoshimura, Y., Ikeda, R. (JAEA),
Nagasaki, K., Yamamoto, S., Ohshima, S., Sano, F., Mizuuchi, T., Okada, H., Minami, T., Kobayashi, S. (Kyoto Univ.)

EBW heating experiments were carried out in the Heliotron J using 2.45-GHz electron cyclotron resonance heating (ECRH). The purpose of the research is (1) production of over-dense plasma of which electron density exceeds the microwave cut off, (2) clarification of a mechanism of microwave mode conversion process to electron Bernstein wave (EBW) and the EBW heating characteristics on toroidal plasmas and (3) deepening the physical understandings of plasma transport and the MHD characteristics in the over-dense plasmas.

Figure 1 shows the poloidal magnetic surface at the toroidal angle where (a) the 2.45-GHz electron cyclotron wave (ECW) was injected and (b) the Langmuir probe was inserted, in the EBW experiments in the Heliotron J. The O-mode ECW was injected with the incident angle to the magnetic surface of 45 deg. In the condition, the EBW experiments with the mode conversion scenario of O-X-B and/or X-B can be carried out. The magnetic field strength was set 650 G on the magnetic axis and the fundamental resonance surface was located close to the last closed flux surface (LCFS).

Figure 2 shows the dependence of the normalized electron density $\langle n_e \rangle / n_{ec}$ on the normalized toroidal magnetic field B_{axis}/B_{res}, where $\langle n_e \rangle$ is the line-averaged-electron density, n_{ec} is the cutoff density of 7.4×10^{16} m^{-3}, B_{axis} and B_{res} are magnetic field strength on the magnetic axis and that on the ECH resonance surface, respectively. The ECW was injected with 15 kW and the fueling gases are deuterium and neon. Higher electron density was obtained in the case of B_{axis}/B_{res} ~74% than that in ~86%. This is considered due to the difference of the process of the mode conversion and the absorption to plasma between them. The achieved $\langle n_e \rangle / n_{ec}$ reached 10 in Ne plasmas, on the other hands, that was at most 4 in D_2. One of the candidates to explain this result is that the effective collisional damping was realized in Ne plasmas because the collision frequency of Ne is considerably higher than that of D_2. Note that the characteristics of the particle and energy transport were also considered to be different in Ne and D_2 plasmas.

Figure 3 shows the radial profiles of the electron temperature T_e, n_e and the absorbed ECW power δP_{abs}, which was evaluated using the ECW-power-modulation technique, under (a) B_{axis}/B_{res} = 86% and (b) 74% in Ne plasmas. As can be seen in fig.3 (a), n_e profile became broad with the central value of 4 times larger than n_{ec}, however, δP_{abs} showed hollow profile leading to the hollow T_e profile in the case of B_{axis}/B_{res} = 86%. The volume integral of the absorption ratio was small value of only 12%. On the other hands, strongly center-peaked deposition profile was realized in the case of B_{axis}/B_{res} = 74%. The center peaked n_e profile with the very high central value of 27 times larger than n_{ec} was obtained. The volume integral of the absorption ratio was significantly higher than that in B_{axis}/B_{res} = 86% and the value reached 66%.

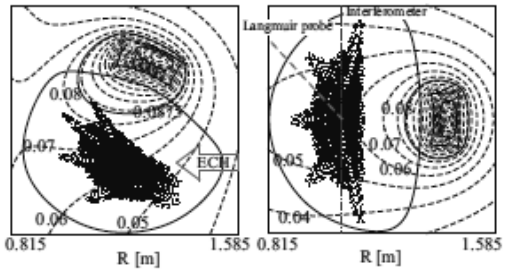

Figure 1. The poloidal magnetic surface at the toroidal angle where (a) the 2.45-GHz ECW was injected and (b) the Langmuir probe was inserted.

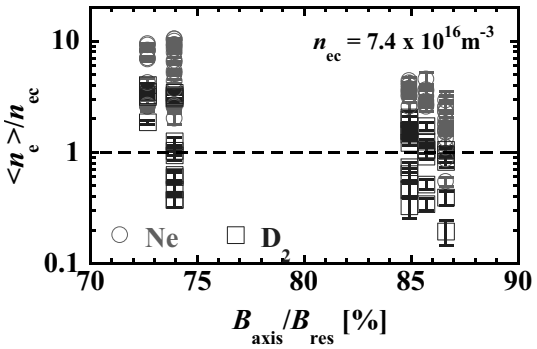

Figure 2. The dependence of $\langle n_e \rangle / n_{ec}$ on B_{axis}/B_{res}.

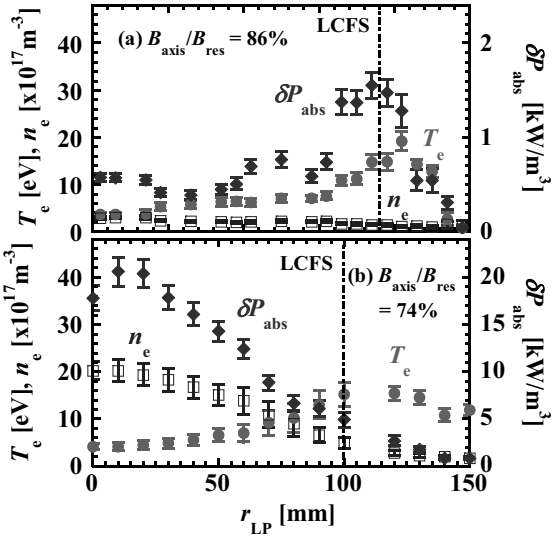

Figure 3. The radial profiles of T_e, n_e and δP_{abs} under (a) B_{axis}/B_{res} = 86% and (b) 74% in Ne plasmas.